

Document downloaded from:

<http://hdl.handle.net/10251/101839>

This paper must be cited as:



The final publication is available at

<https://doi.org/10.1016/j.jnoncrysol.2006.11.003>

Copyright Elsevier

Additional Information

# Poly(ethyl methacrylate – co - hydroxyethyl acrylate) random copolymers: dielectric and dynamic-mechanical characterisation

J.A. Gómez-Tejedor<sup>a\*</sup>, T. Rodríguez Acosta<sup>b</sup>,  
J.L. Gómez Ribelles<sup>b,c</sup>, G. Polizos<sup>d</sup>, P.Pissis<sup>d</sup>

<sup>a</sup>Centre for Biomaterials and Dept. of Applied Physics, Universidad Politécnica de Valencia, ETS de Informática Aplicada, E-46022 Valencia, Spain

<sup>b</sup>Centre for Biomaterials and Dept. of Applied Thermodynamics, Universidad Politécnica de Valencia, P.O. Box 22012, E-46071 Valencia, Spain

<sup>c</sup>Centro de Investigación Príncipe Felipe, Avda. Autopista del Saler 16, 46013 Valencia, Spain

<sup>d</sup>National Technical University of Athens, Department of Physics, Zografou Campus, 15780 Athens, Greece

## Abstract

The conformational mobility in poly(ethyl methacrylate – co – hydroxyethyl acrylate) copolymers was studied by dielectric relaxation spectroscopy, thermally stimulated depolarisation currents and dynamic-mechanical experiments. The relaxation strength and the shape of the dielectric relaxation spectra of the homopolymer and copolymer networks were analysed using the Havriliak-Negami equation. The dependence of the relaxation strength on copolymer composition and temperature was analysed taking into account the merging of the main and the secondary relaxation processes. The shape of the  $\epsilon''$  vs frequency plots led to the conclusion that the distribution of relaxation times was broader in the copolymers with

---

\* Corresponding author

Email address: jogomez@fis.upv.es (J.A. Gómez-Tejedor).

intermediate composition than in the homopolymers, a feature that can be explained by the inhomogeneity produced at molecular scale by the sequence distribution of the monomeric units along the chain. Master curves were built both for the elastic modulus and the mechanical loss tangent, and the temperature dependence of the relaxation times was deduced from the shift factors. The fit to the Vogel equation permitted the calculation of the strength parameter, which is higher in the copolymers than the simple average of the values of the homopolymers, a feature that can be related to the broadness of the distribution of relaxation times.

**PACS Codes:** 36.20.-r 82.35.Jk

**Key words:** copolymer C274; polymer network P297; dielectric relaxation D185, dynamical properties D270, Mechanical Properties M120

## 1 Introduction

Random copolymers present a single glass transition situated at temperatures between those of the corresponding homopolymers. The dependence of the glass transition temperature,  $T_g$ , on the copolymer composition usually corresponds to quite simple equations [1-3] that can be deduced on thermodynamic or free volume grounds. The monomer sequence distribution, determined by the reactivity ratios, also may affect the glass transition temperature due to the change in the interactions between adjacent monomeric units along the chain. This effect can be enhanced when one of the monomers presents a strong permanent dipolar moment while the other is not polar [4,5]. The influence of this effect on the composition dependence of  $T_g$  can also be taken into account in the empirical equations [6,7]. Moreover, a very different reactivity of the monomers can produce long sequences of a monomeric unit capable of associating and form domains that undergo its own glass transition, as is the case of poly(ethyl acrylate – co – hydroxyethyl methacrylate), in which free radical polymerisation produces a nanophase separation of hydrophobic domains in a copolymer hydrophilic matrix

[8]. Nevertheless, the glass transition temperature is a limited characterisation of the vitrification process. The glass transition occurs because of the rapid increase of the relaxation times of the co-operative conformational rearrangements of the polymer chain segments in a more or less narrow temperature interval. In this work the segmental dynamics of poly(ethyl methacrylate-co-hydroxyethyl acrylate) random copolymers was analysed using dielectric spectroscopy and dynamic-mechanical analysis in the temperature interval of the main relaxation or  $\alpha$  process. This allows for a deeper insight into the study of the influence of composition on the conformational mobility of the copolymer.

The molecular mobility of poly(alkyl methacrylate)s has been extensively studied using dielectric relaxation spectroscopy. All the way back in 1966, Williams [9] stated that the main  $\alpha$  relaxation and the secondary  $\beta$  relaxation merge at temperatures above the glass transition temperature  $T_g$ , in a new  $\alpha\beta$  relaxation process which has characteristics different from both  $\alpha$  and  $\beta$  relaxation, i.e. it is not a mere superpositioning of both processes. The crossover region is the frequency-temperature region in which the relaxation times of the  $\alpha$  and  $\beta$  processes approach each other. An extensive analysis of the knowledge and different viewpoints for evaluating the contribution of each component to the overall relaxation process can be found in references [10,11]. The merging of the main and the secondary dielectric relaxations may well be a general phenomenon in amorphous polymers, as proven using broadband dielectric spectroscopy [12,13]. The relative strength of the secondary and the main relaxation determines the shape of the relaxation spectrum and the measured temperature dependence of the relaxation strength. The main dielectric relaxation predominates on the  $\beta$  relaxation in the polymers of the series of poly(n-alkyl acrylates) and thus it is possible to obtain a quite precise analysis of its behaviour [14]. On the contrary, a significant contribution of the  $\beta$  relaxation is present in the merging zone of PEMA [15]. In the case of viscoelastic behaviour, the main relaxation always predominates in the secondary relaxations. In this way an experimental analysis using both dielectric and dynamic-mechanical experiments can give quite a

complete picture of the segmental dynamics of P(EMA-co-HEA) random copolymers.

## 2 Experimental

### 2.1 Materials

Monomers: ethyl methacrylate, EMA, (Aldrich, 99% pure) and hydroxyethyl acrylate, HEA, (Aldrich, 96% pure) were used without further purification. The polymer networks were synthesised by free radical addition polymerisation using as a photo-initiator 0.2% by weight of benzoin (Merk, 98% pure) and adding 1% by weight of ethylene glycol dimethacrylate, EGDMA, as a cross-linking agent (Merck, 98% pure). The cross-links prevent permanent flow above the glass transition, allowing DMA experiments across glass-transition to be performed. The monomer, cross-linking agent and initiator were used as received without further purification. Polymerisation took place at room temperature for 24 hrs under UV radiation. Low molecular weight substances remaining in the samples after polymerisation were extracted from the polymer network by boiling in ethanol for 12 hrs and then drying in vacuo at 90°C until the weight remained constant (around 72 hrs). In this way, pure poly(ethyl methacrylate), PEMA, pure poly(hydroxyethyl acrylate), PHEA, and a series of copolymers with varying EMA and HEA contents were obtained. The copolymers will be designed as P(EMA-co-HEA)XX/YY, XX and YY being the weight fraction of EMA and HEA units respectively.

### 2.2 TSDC experiments

For thermally stimulated depolarisation currents (TSDC), a dielectric technique in the temperature domain [16-18], a Novocontrol TSDC cell and a cryostatic system were used. The sample was clamped between two golden electrodes. The depolarisation current was measured by means of a Keithley 617 electrometer as a function of temperature in the range from about -100 to about 150°C. The TSDC

method consists of measuring the thermally activated release of stored dielectric polarisation and corresponds to measuring dielectric losses versus temperature at constant low frequencies of  $10^{-4}$  to  $10^{-2}$  [16-18]. As a result of these low frequencies, TSDC is characterised by high sensitivity and high resolving power. The sample is placed between the plates of a capacitor and polarised by the application of an electric field between 4000 and 5000 V/cm at a suitably chosen polarisation temperature (see below) for 4 minutes, quite a long time compared to the relaxation time of the relaxation under investigation at the polarisation temperature. Then, with the electric field applied, the sample is cooled at 8-10°C/min to a sufficiently low temperature to prevent depolarisation by thermal excitation, about 100K using our measurements. The field is then switched off and the sample is heated at a constant heating rate of 3-4°C/min. A discharge current is generated as a temperature function, which is measured with a sensitive electrometer. As temperature increases, the molecular groups where permanent dipolar moments reside acquire sufficient mobility, giving an inherent current peak for each polarisation mechanism, whose shape and location is characteristic of the relaxation mechanisms of the sample.

### 2.3 DRS experiments

The Dielectric Relaxation Spectroscopy (DRS) experiments were performed with a Schlumberger frequency response analyzer SI1260 in combination with a cryostatic Novocontrol System. Samples with square geometry and adequate dimensions to fit in the 20 mm diameter electrode were used. In these experiments, the complex relative dielectric permittivity  $\epsilon^* = \epsilon' - i\epsilon''$  was determined as a function of frequency ( $10 - 10^7$  Hz) in different temperature ranges depending on the glass transition temperature and conductivity of the sample: from 0°C to 100°C for pure PHEA and from 70°C to 160°C for pure PEMA.

## 2.4 DMA experiments

The dynamic mechanical analysis (DMA) experiments were performed in a Seiko DMS210 analyser both under isothermal and non-isothermal conditions for all the samples in the extension mode. Prismatic samples approximately  $6 \times 0.6 \times 10.0 \text{ mm}^3$  were used. The heating scans were carried out at 1 Hz at a heating rate of  $1^\circ\text{C}/\text{min}$ . The isothermal experiments were carried out in the glass transition region of the samples every  $2^\circ\text{C}$ . At each temperature the frequency was scanned from 0.01 to 20 Hz.

## 3 Results

### 3.1 TSDC experiments

The intensity of TSDC relaxation depends on the thickness of the samples and the heating rate. For this reason the comparison of thermograms is not possible without prior normalisation. The normalised intensities are calculated according to the expression:

$$I_n = \frac{Id}{Vb}$$

Where  $I$  is the measured intensity in Ampere,  $b$  the heating rate in  $\text{deg}/\text{min}$ , and  $V/d$  the polarising field ( $V$  in Volt and  $d$  is the thickness of the sample).

The normalised depolarisation current for each sample is shown in Figure 1. The polarisation temperatures were:  $90^\circ\text{C}$  for PEMA, P(EMA-co-HEA)80/20 and P(EMA-co-HEA)60/40,  $40^\circ\text{C}$  for P(EMA-co-HEA)50/50 and  $30^\circ\text{C}$  for P(EMA-co-HEA)20/80 and PHEA.

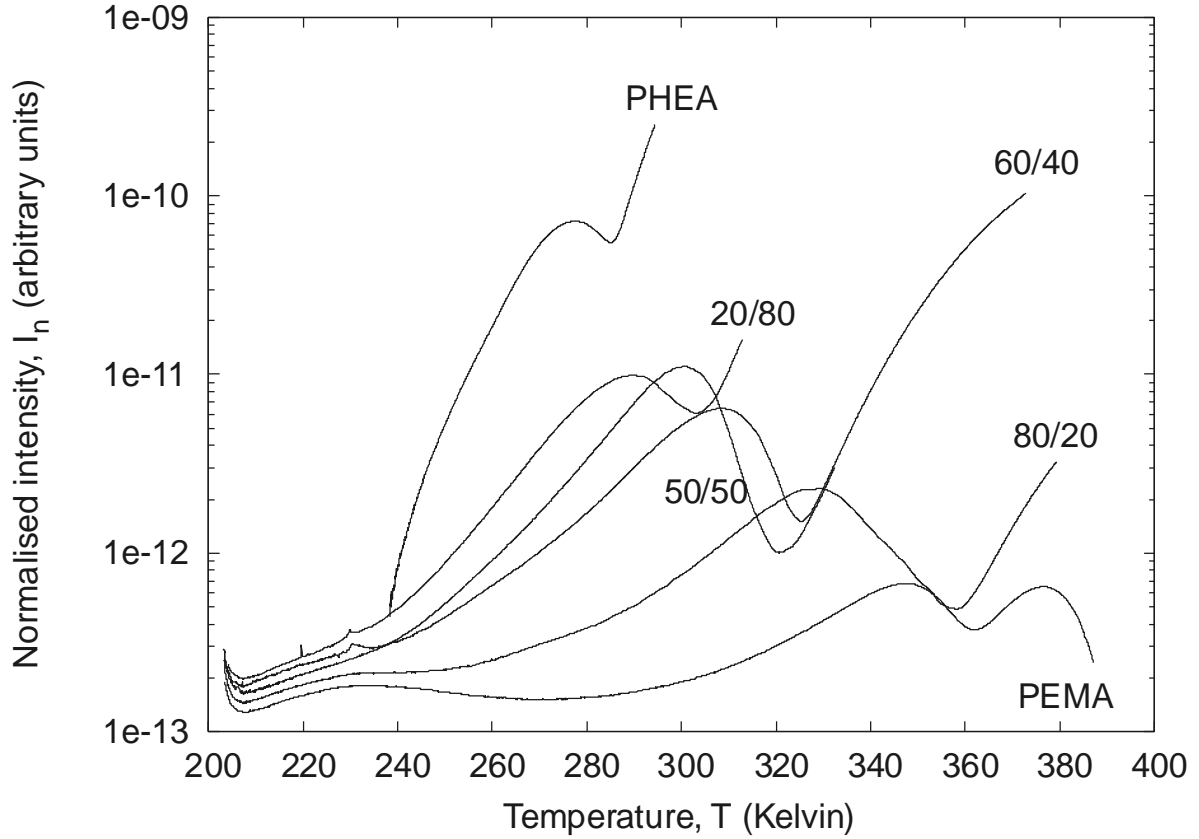


**Figure 1.** Normalised TSDC thermograms measured for all the samples indicated on the plot. The polarisation temperatures are: 90°C for PEMA, P(EMA-co-HEA)80/20 and P(EMA-co-HEA)60/40, 40°C for P(EMA-co-HEA)50/50 and 30°C for P(EMA-co-HEA)20/80 and PHEA.

The composition dependence of the temperature of the maximum,  $T_{\alpha TSDC}$ , fits very well to the Fox equation [2] as shown in Figure 2

$$\frac{1}{T_{\alpha, TSDC}^{cop}} = \frac{w_{HEA}}{T_{\alpha, TSDC}^{PHEA}} + \frac{1 - w_{HEA}}{T_{\alpha, TSDC}^{PEMA}} \quad (1)$$

where  $T_{\alpha, TSDC}^{cop}$ ,  $T_{\alpha, TSDC}^{PHEA}$ ,  $T_{\alpha, TSDC}^{PEMA}$  are the temperatures of main relaxation of the copolymer, and pure PHEA and PEMA homopolymer networks respectively, and  $w_{HEA}$  is the weight fraction of HEA units in the copolymer network.



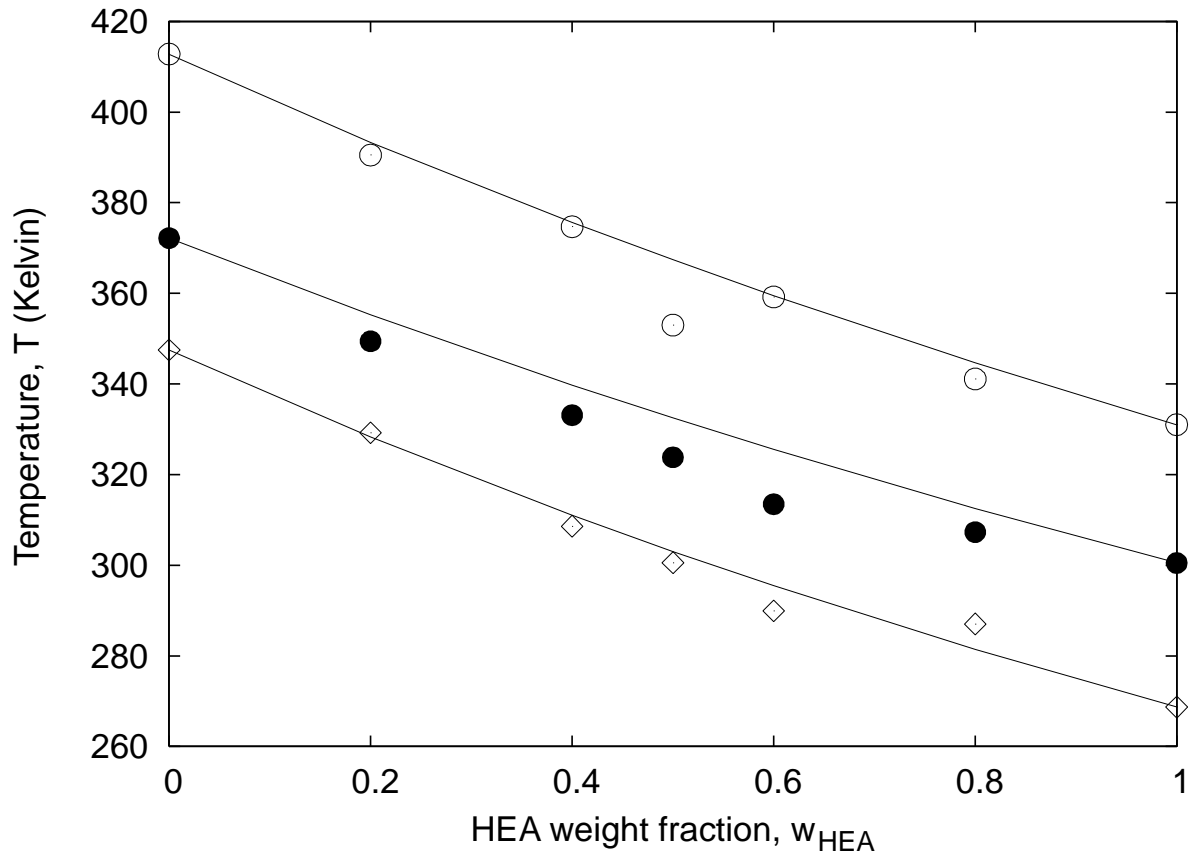


**Figure 2.** Temperatures of main relaxation of the copolymer as a function of the weight fraction of HEA units in the copolymer network. (◇) Maximum of the TSDC peak corresponding to the  $\alpha$  relaxation, (○) Temperature of the  $\varepsilon''$  peak at  $10^5$  Hz, (●) Glass transition temperature determined from the dynamic-mechanical master curves as the temperature at which the mechanical relaxation time equals 100 seconds. The solid lines represent the Fox equation result.

### 3.2 DRS experiments

The dielectric measurements carried out isothermally in a broad temperature interval in the series of homopolymer and copolymer networks supply complete data sets of the temperature and frequency dependences of the real and imaginary parts,  $\varepsilon'$  and  $\varepsilon''$  of the complex relative dielectric permittivity. From the latter the evolution of the ac conductivity ( $\sigma_{ac}$ ) can also be obtained through

$$\sigma_{ac}(f) = \varepsilon''(f)\varepsilon_0 2\pi f \quad (2)$$

where  $\varepsilon_0$  is the permittivity of free space.

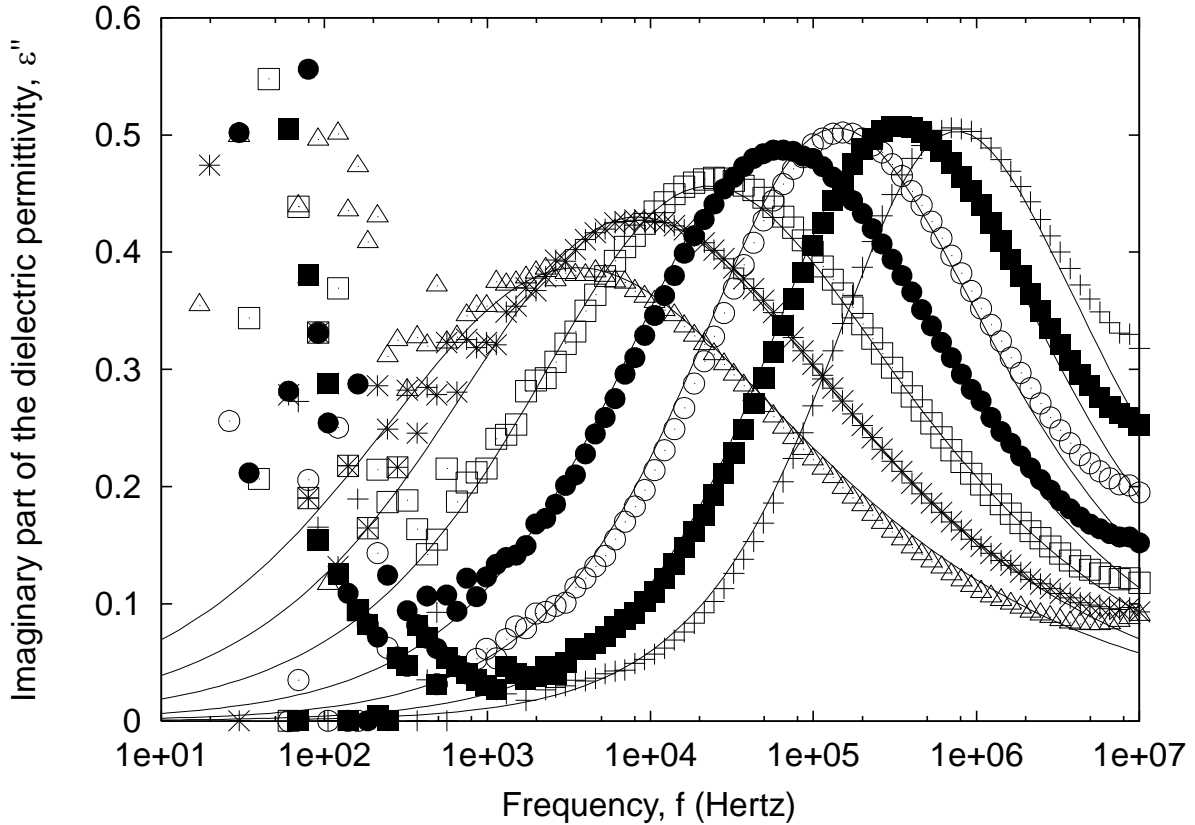


**Figure 3.** Frequency dependence of  $\varepsilon''$  measured in PEMA: ( $\Delta$ ) 100°C, ( $*$ ) 110°C, ( $\square$ ) 120°C, ( $\bullet$ ) 130°C, ( $\circ$ ) 140°C, ( $\blacksquare$ ) 150°C and ( $+$ ) 160°C. The solid line represents the Havriliak-Negami fit.

Only a few representative data results are presented here. Figure 3 presents  $\varepsilon''$  in the frequency domain for several isotherms of PEMA network. As a representative example of the DRS results obtained in the copolymers, Figure 4 shows the plots of  $\varepsilon''$  for different temperatures. The temperature range of the measurements covers mainly the main,  $\alpha$ , relaxation zone. The increase of  $\varepsilon''$  in the high

frequency side of the peak should correspond to the overlapping of the secondary,  $\beta$ , relaxation present in both components. On the other hand the increase of  $\varepsilon''$  in the low frequency side with decreasing frequency corresponds to the dc conductivity contribution. The dc conductivity of the polymer can be characterised by the temperature dependence of the limit of  $\sigma_{ac}$  to low frequencies, as shown in Figure 5 for the copolymer series.

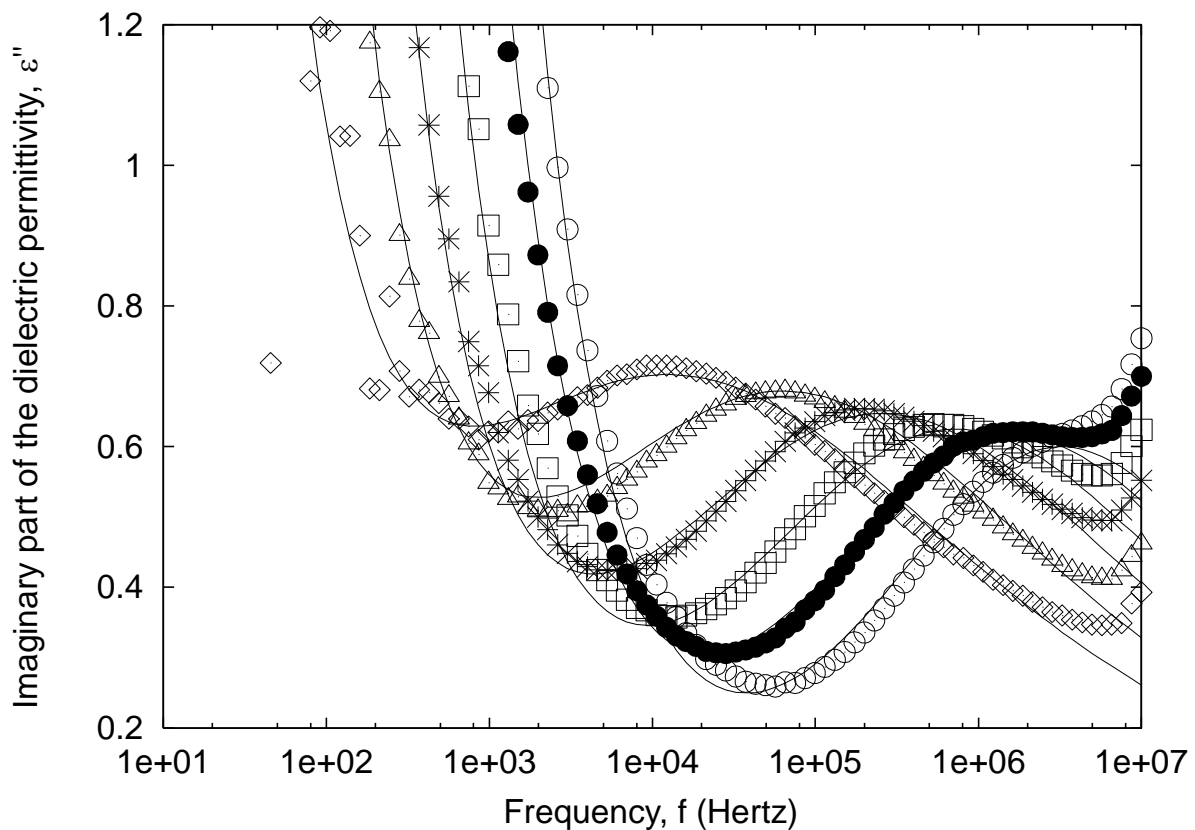


**Figure 4.** Frequency dependence of  $\varepsilon''$  measured in P(EMA-co-HEA)60/40: ( $\diamond$ ) 90°C, ( $\triangle$ ) 100°C, ( $\ast$ ) 110°C, ( $\square$ ) 120°C, ( $\bullet$ ) 130°C, and ( $\circ$ ) 140°C . The solid line represents the Havriliak-Negami fit.

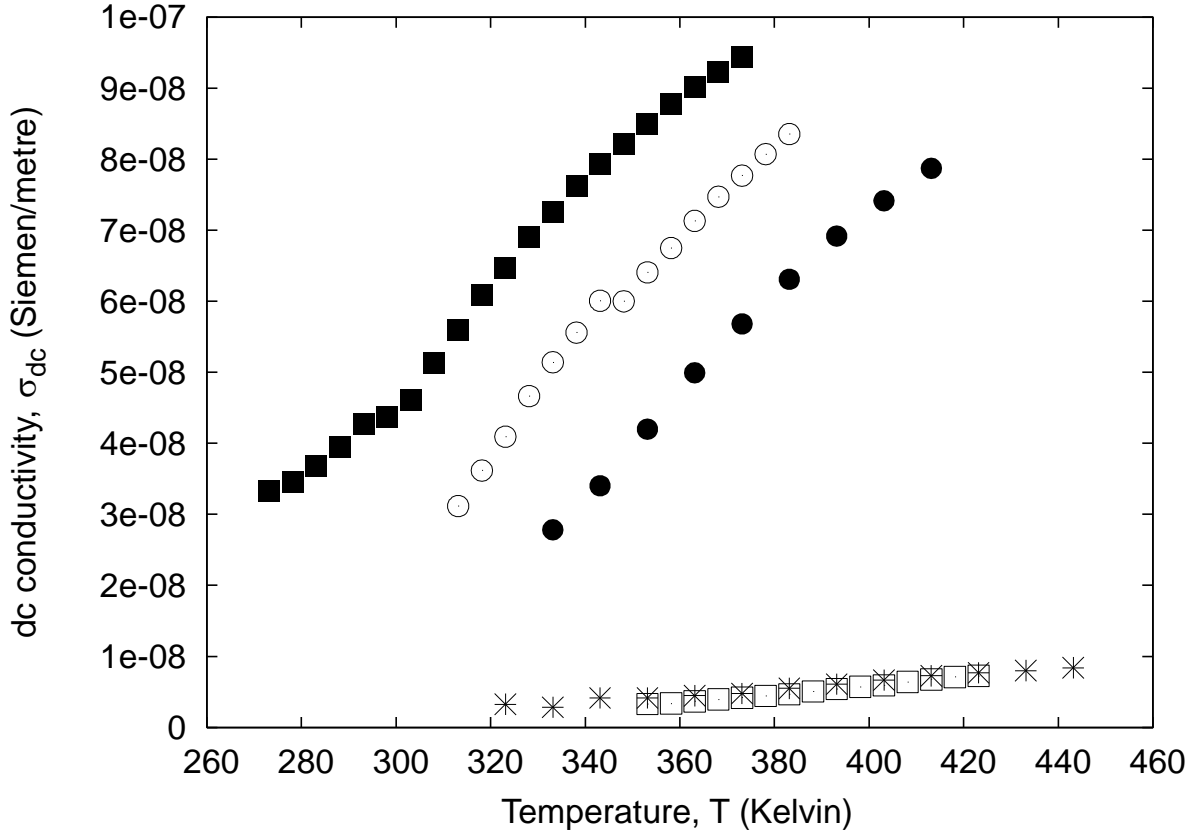


**Figure 5.** dc conductivity for homopolymer and copolymer networks: (✱)P(EMA-co-HEA)60/40, (□)P(EMA-co-HEA)50/50, (●)P(EMA-co-HEA)40/60, (○)P(EMA-co-HEA)20/80 and (■) PHEA.

Empirical functions have commonly been used to analyse the shape of the dielectric relaxation. In our case, the following expression has been used to fit the experimental dielectric loss data [19,20]:

$$\varepsilon''(\omega) = \Delta\varepsilon \frac{\sin(b\phi)}{\left\{1 + 2(\omega\tau_0)^{1-a} \sin\left(\frac{1}{2}a\pi\right) + (\omega\tau_0)^{2(1-a)}\right\}^{\frac{b}{2}}} + \frac{\sigma}{\varepsilon_0} \omega^{-s} \quad (3)$$

where

$$\phi = \arctg \left[ \frac{(\omega\tau_0)^{1-a} \cos\left(\frac{1}{2}a\pi\right)}{1 + (\omega\tau_0)^{1-a} \sin\left(\frac{1}{2}a\pi\right)} \right] \quad (4)$$

The first term of equation (3) is the Havriliak-Negami (HN) equation [21,22].  $\Delta\varepsilon$  is the relaxation strength, and  $f_0=1/(2\pi\tau_0)$  is a characteristic frequency, approximately equal to the  $\varepsilon''$  maximum frequency,  $f_{max}$ [19, 21]:

$$f_{max} = f_0 \left[ \frac{\sin\left[\frac{(1-a)\pi}{2+2b}\right]}{\sin\left[\frac{(1-a)b\pi}{2+2b}\right]} \right]^{1/(1-a)} \quad (5)$$

The second term of equation 3 is the conductivity contribution to  $\varepsilon''(\omega)$ ,  $\sigma$  is a constant, and the exponent  $s$  is less than or equal to 1.

The exponent  $a$  represents the relaxation peak width, while the parameter  $b$  is related to the symmetry of the relaxation  $[0 < (1-a), (1-a)b \leq 1]$ . The fit of the model equations to the experimental results requires certain simplifivative assumptions due to the correlation between the different fitting parameters. The value of  $\varepsilon_\infty$  was assumed to be temperature independent and the parameter  $b$  was also considered temperature independent since its value was found to change only slightly and not systematically with temperature. With these assumptions, the fit to all the isotherms in all the copolymers is quite good. The solid lines in Figures 3 and 4 exemplify this. Table 1 shows the values of these parameters for the different samples. The temperature dependence of the relaxation strength and of parameter  $a$  are shown in Figure 6. All fits have been done using an implementation of the nonlinear least-squares Marquardt-Levenberg algorithm. Parameter errors have been obtained from the variance-covariance matrix after the final iteration.

**Table 1.**

Characteristic parameters of the main relaxation processes of copolymer networks:  $b$  and  $\varepsilon_\infty$  parameters from the Havriliak-Negami equation; glass transition temperature  $T_g$  determined as the temperature at which the mechanical relaxation time equals  $\tau=100$  s.;  $B$  and  $T_0$  parameters of the VFTH equation and strength parameter  $D=B/T_0$ .

	PEMA	P(EMA-co-HEA) 80/20	P(EMA-co-HEA) 60/20	P(EMA-co-HEA) 50/50	P(EMA-co-HEA) 40/60	P(EMA-co-HEA) 20/80	PHEA
$b$	$0.650 \pm 0.012$	$0.65 \pm 0.03$	$0.65 \pm 0.05$	$0.65 \pm 0.05$	$0.65 \pm 0.06$	$0.65 \pm 0.07$	
$\varepsilon_\infty$	$2.60 \pm 0.04$	$3.30 \pm 0.19$	$3.9 \pm 0.3$	$3.9 \pm 0.4$	$4.0 \pm 0.6$	$6.0 \pm 0.8$	
$T_g$ (K)	$372.2 \pm 0.2$	$349.4 \pm 0.2$	$333.1 \pm 0.2$	$323.8 \pm 0.2$	$313.5 \pm 0.2$	$307.3 \pm 0.2$	$300.5 \pm 0.2$
$B$ (K)	$1070 \pm 40$	$990 \pm 30$	$970 \pm 40$	$1040 \pm 150$	$752 \pm 14$	$635 \pm 19$	$490 \pm 110$
$T_0$ (K)	$281.0 \pm 1.8$	$262.5 \pm 1.4$	$249.6 \pm 1.8$	$236 \pm 8$	$244.8 \pm 0.8$	$239.4 \pm 1.2$	$243 \pm 8$
$D$	$3.81 \pm 0.17$	$3.77 \pm 0.13$	$3.89 \pm 0.19$	$4.3 \pm 0.8$	$3.07 \pm 0.07$	$2.65 \pm 0.09$	$2.0 \pm 0.5$

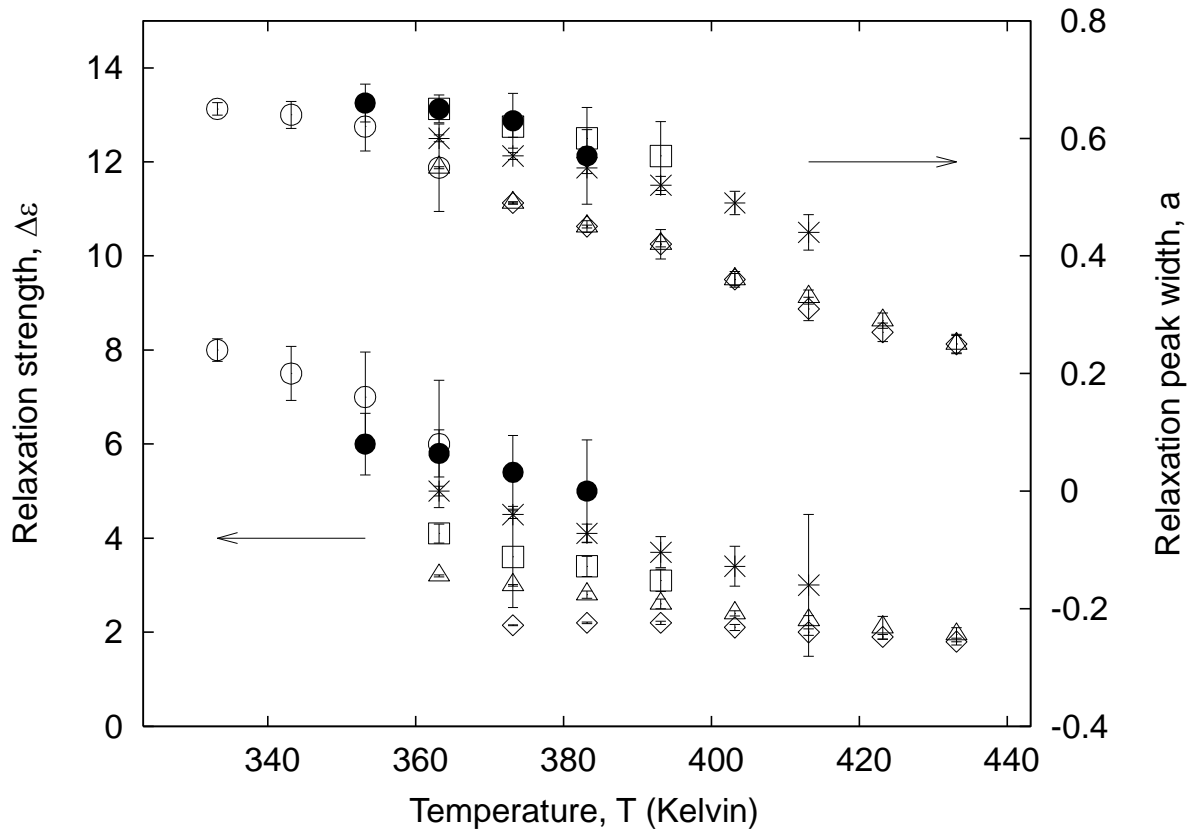
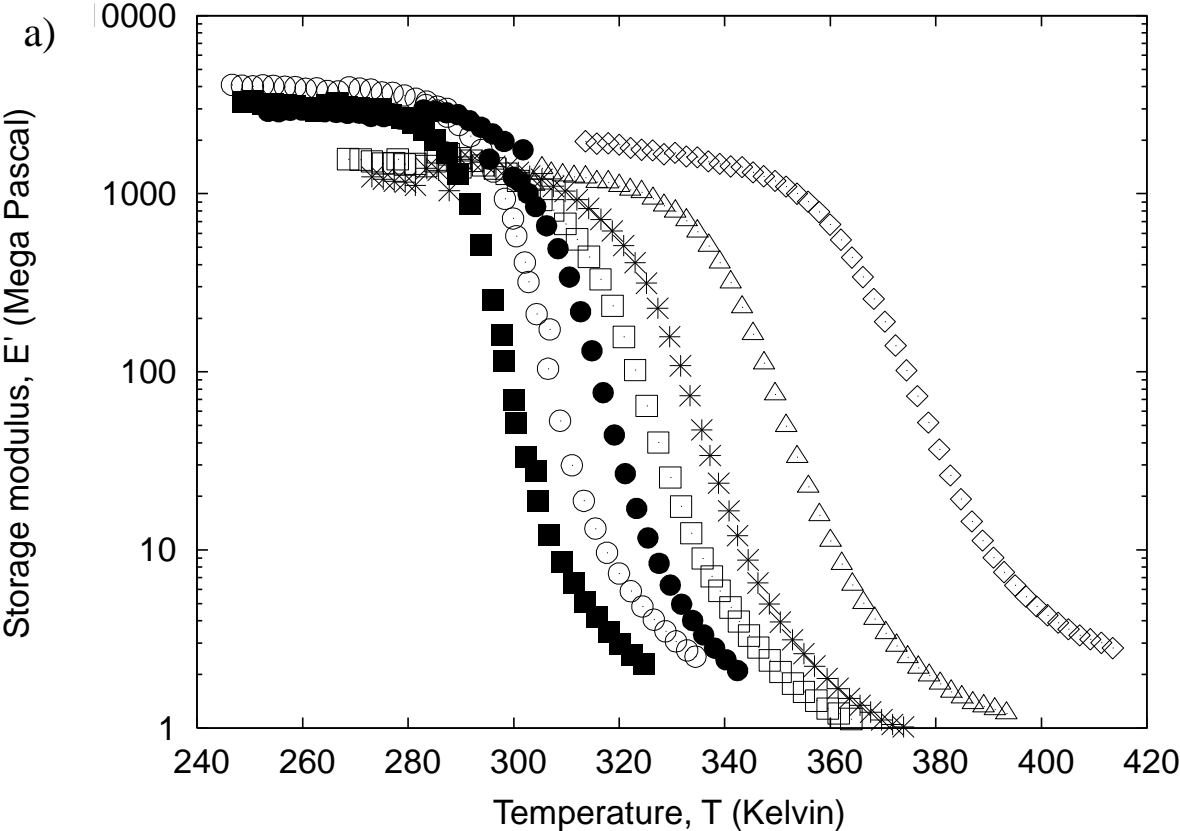


**Figure 6.** Temperature dependence of the relaxation strength and of parameter  $a$  in Havriliak-Negami equation: ( $\diamond$ ) PEMA, ( $\triangle$ )P(EMA-co-HEA)80/20, ( $*$ )P(EMA-co-HEA)60/40, ( $\square$ )P(EMA-co-HEA)50/50, ( $\bullet$ )P(EMA-co-HEA)40/60 and ( $\circ$ )P(EMA-co-HEA)20/80.

### 3.3 DMA experiments

The temperature dependence of the loss tangent and storage modulus measured in isochronal DMA scans of the analysed samples in the  $\alpha$ -relaxation region are presented in Figure 7, where it can be seen how the mechanical relaxation progressively shifts towards higher temperatures as the HEA content in the copolymer decreases, while the peak broadens and the maximum value of the loss tangent decreases. The temperature for the maximum of the loss tangent in this representation can be called the temperature of the main dynamic-mechanical relaxation,  $T_{\alpha DMA}$ . Figure 2 shows the dependence of  $T_{\alpha DMA}$  on copolymer

composition. The prediction of equation (1) expressed for  $T_{\alpha DMA}$  instead of  $T_{\alpha TSDC}$  is also represented as a solid line. In this case the relaxation position predicted by the Fox model is higher than the experimental values in the whole composition interval.





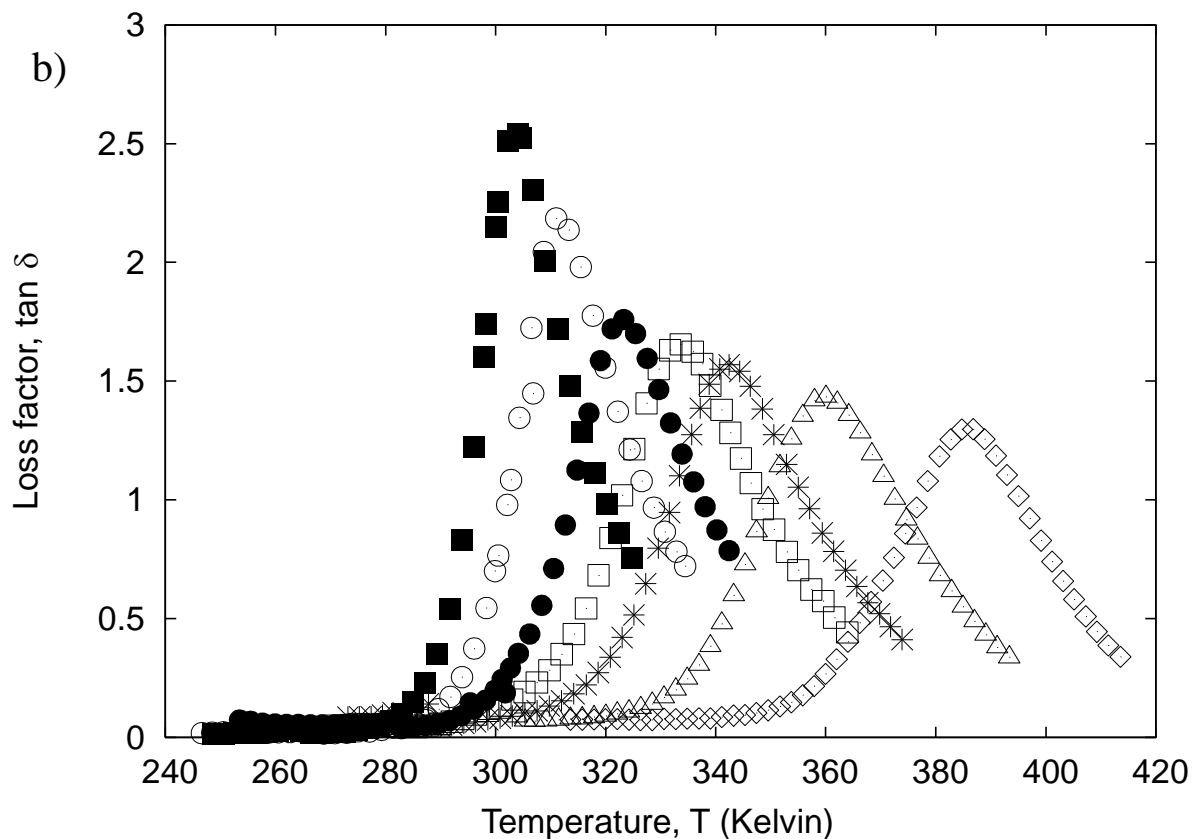


**Figure 7.** Temperature dependence of the storage modulus ( $E'$ ) (a) and loss factor ( $\tan \delta$ ) (b) for homopolymer and copolymer networks : ( $\diamond$ ) PEMA, ( $\triangle$ )P(EMA-co-HEA)80/20, ( $*$ )P(EMA-co-HEA)60/40, ( $\square$ )P(EMA-co-HEA)50/50, ( $\bullet$ )P(EMA-co-HEA)40/60, ( $\circ$ )P(EMA-co-HEA)20/80 and ( $\blacksquare$ ) PHEA.

From the isothermal scans measured in the temperature interval around  $T_g$ , master curves for storage modulus ( $E'$ ) and loss factor ( $\tan \delta$ ) were obtained by superposition on the isotherm corresponding to  $T_g$  for all the samples (Figure 8). In order to build the master curves, the squared distance between two consecutive curves in the intersection region was calculated (both at the same time, storage modulus and loss factor) to find the shift factor that minimises this distance.

The method for determining the glass transition temperature in each sample was as follows. First, the master curves for storage modulus and loss factor were built

using an arbitrary reference temperature  $T_{ref}$ , obtaining in this way the shift factors  $a_T$  for each temperature. After this, the storage modulus was fitted to the Kohlrausch-Williams-Watts (KWW) equation:

$$E'(f * a_T) = E'_0 + (E'_{inf} - E'_0) \left( 1 - \exp \left( - \left( \frac{f * a_T}{\tau(T_{ref})} \right)^{\beta_{KWW}} \right) \right)$$

where  $E'_0$  and  $E'_{inf}$  represent the storage modulus for low and high frequencies respectively. The  $\beta_{KWW}$  parameter is associated with the distribution of characteristic times, and  $\tau(T_{ref})$  is the KWW relaxation time at the chosen reference temperature. Then, from the evaluated shift factors, the relaxation time for each temperature was calculated using  $\log \tau(T) = \log a_T + \log \tau(T_{ref})$ .

The glass transition temperature was defined as the temperature at which the relaxation time is equal to 100 s. This glass temperature is shown on Table 1 for all the samples.

Finally, the master curves were redrawn using the glass transition temperature as the reference temperature for superposition. These curves are represented in Figure 8.

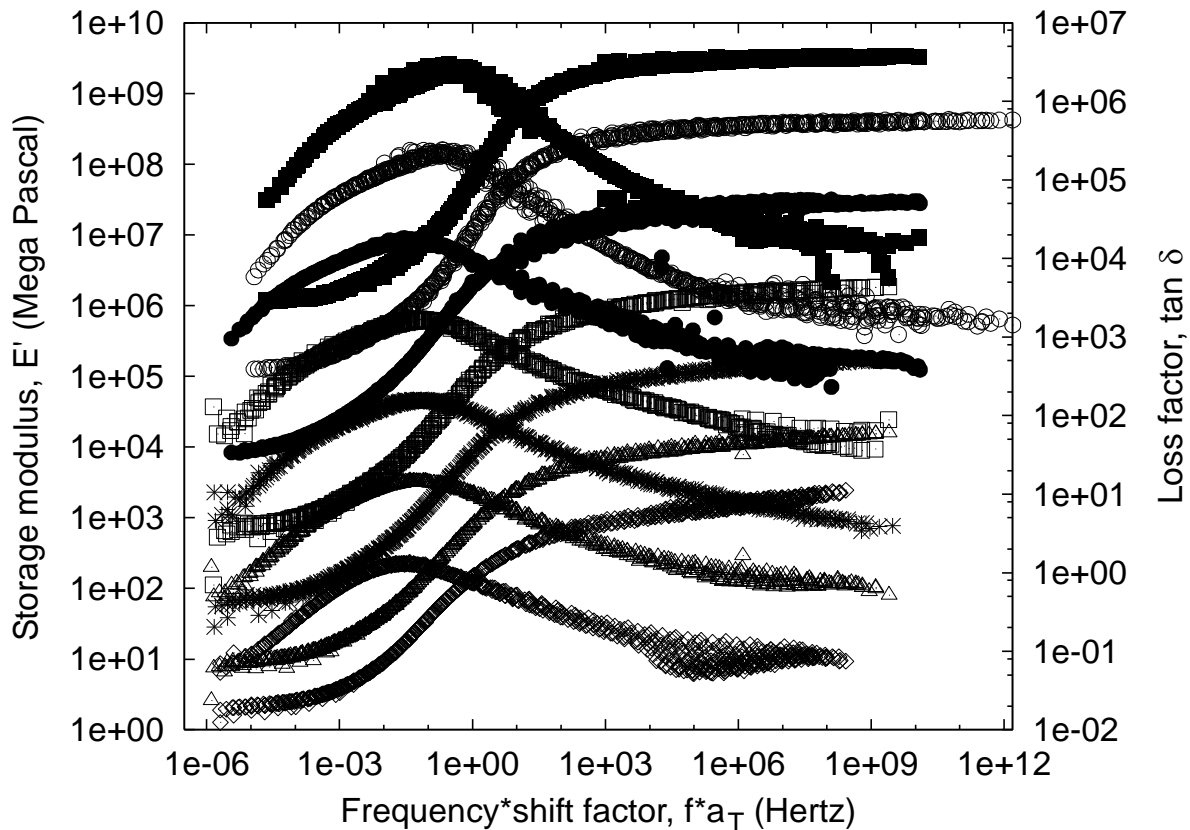


**Figure 8.** Storage modulus ( $E'$ ) and loss factor ( $\tan \delta$ ) master curves, using  $T_g$  as the reference temperature for superposition, for copolymers samples with different phea/pema concentration. Starting from the P(EMA-co-HEA)80/20 curve, the curves have been shifted one unit in the Y axis with respect to the previous one. Symbols as in Figure 7.

The superposition of the different isotherms was achieved by simple shifting of the isothermal results along the  $\log f$  axis, according to the time-temperature superposition principle [24]. The criterion was that the same shift applied for both the  $\log E'$  and  $\tan \delta$  plots. The latter was preferred to the  $\log E'$  curves because in poly(alkyl methacrylates) the isothermal plot of  $E''$  does not present a peak due to the width of the transition and the  $\alpha$ - $\beta$  merging. In this case, the vertical shift due to the temperature dependence of the product  $\rho T / \rho T^*$  [24] seems to be negligible.

The temperature dependence of the relaxation times was successfully described by the Vogel-Fulcher-Tamman-Hesse equation (VFTH) [26-29] (see Figure 9):

$$\tau(T) = \tau_0 \exp \frac{B}{T - T_0}, \quad (7)$$

where  $\tau_0$  is a pre-exponential factor and the values of the adjustable parameters  $B$  and  $T_0$  for the different networks are listed on Table 1.

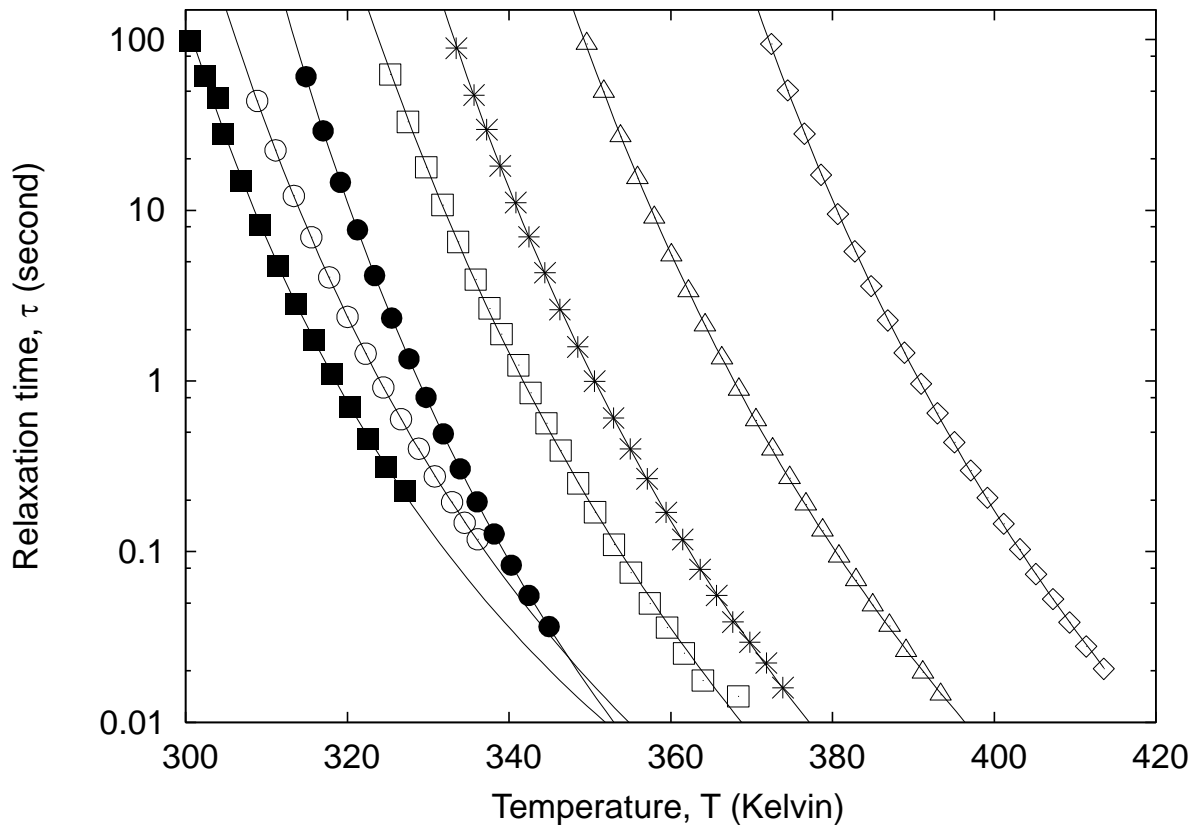


**Figure 9.** Temperature dependence of the viscoelastic relaxation times defined as the  $\tau$  constant in the KWW equation. The fit to VFTH equation is represented by the solid lines. Symbols as in Figure 7.

## 4 Discussion

Both in dielectric and dynamic-mechanical spectroscopy results, one single main relaxation peak is shown by the copolymers, indicating that free radical polymerisation produced a homogeneous copolymer phase. Although the polar groups along the chains were not randomly distributed due to differences in the reactivity of both monomers, there is no sign of aggregation of polar or non-polar groups with dimensions that would be sufficient to produce independent glass transitions.

The TSDC thermogram corresponding to pure PEMA, the most hydrophobous polymer of the series, presents the secondary  $\beta$  relaxation at low temperatures, followed by the main  $\alpha$  relaxation, around 75°C, due to the cooperative conformational rearrangements of the polymer segments and, at the highest temperatures, the  $\rho$  peak due to space charge motions appears around 100°C. The three relaxation processes have been well described in the PEMA chain polymer [16]. As the content of HEA units in the copolymer increases, the contribution of the space charge relaxation increases due to the increasing water molecules retained in the sample after the drying process. The maximum of the  $\rho$  peak cannot be observed in the temperature range of the measurement, but the rapid increase of the depolarisation current above the  $\alpha$ -relaxation temperature is an indication of the free charge carrier motions in the sample. This contribution produces the apparent increase of the normalised intensity in the temperature interval in which the  $\alpha$  relaxation takes place. Nevertheless, the  $\alpha$  relaxation can be clearly seen even in the case of PHEA homopolymer network.

The main dielectric relaxation in this PEMA is clearly separated from the conductivity contribution at lower frequencies. There is a clear change in the shape of the relaxation with increasing temperature due to the merging of the cooperative  $\alpha$  relaxation and  $\beta$  secondary mechanism in the observed relaxation process. The main features related to the merging of the two mechanisms in the PEMA network have been discussed elsewhere [15] and the general features

related to poly(alkyl methacrylate) polymers have been the subject of several review papers (see references [10,11] and the references cited there).

In the case of the copolymers, the permanent dipolar moment of the hydroxyl group in the side chain increases the strength of the main relaxation and, at the same time, increases the dc contribution, as can be appreciated by the rapid increase of  $\varepsilon''$  when frequency decreases (Figure 4 shows the case of P(EMA-co-HEA)60/40). The investigation of dc conductivity may be utilised for morphological characterisation, as the moving ions probe the local morphology. Two effects contribute to the increase of the conductivity at each temperature with increasing PHEA content shown in Figure 5. The first is a temperature effect, related to the fact that at temperatures above the glass transition temperature  $T_g$ , in the liquid state, conductivity increases with the difference  $T-T_g$  and  $T_g$  decreases with the PHEA content of the copolymer. However, this effect does not explain completely the increase in conductivity shown in Figure 5 as can be proved representing  $\sigma_{dc}$  against  $T-T_g$  or even against  $T/T_g$  (results not shown). The other effect is the higher conductivity of PHEA with respect to PEMA, traces of water may play an important role in this. The results in Figure 5 show that the samples can be classified into two groups. In the first group (P(EMA-co-HEA)60/40 and P(EMA-co-HEA)50/50), the samples are characterised by low values of dc conductivity and weak temperature dependence. In the samples of the second group (P(EMA-co-HEA)40/60, P(EMA-co-HEA)20/80 and PHEA), higher values of dc conductivity combined with strong temperature dependence, which was not quantitatively evaluated here, were observed. Obviously, PHEA becomes the continuous phase in P(EMA-co-HEA)40/60 (and compositions with higher PHEA content), whereas PEMA is the continuous phase in P(EMA-co-HEA)50/50 (and compositions with lower PHEA content).

With the exception of the PEMA network, in which  $\Delta\varepsilon$  goes through a maximum at a temperature close to 120°C, in PHEA and the copolymers the relaxation strength

decreases with increasing temperature, as has been found in the  $\alpha$  and  $\alpha\beta$  relaxation of poly(alkyl-acrylates) and poly(alkyl-methacrylates) [9,11,15]

It is significant that the parameter  $a$  is higher in the copolymers containing 40 and 60% HEA units than in PEMA or the copolymers with a composition close to PEMA and PHEA homopolymers. This means that the relaxation time spectrum of the relaxation broadens in the copolymers, which is possibly due to an increase in composition fluctuations produced by the monomer sequences along the chain. In reference [23] a very simple model was used as an aid to show that random distribution of the chain segments in a two-component system may introduce composition fluctuations in the size of the co-operative length at the glass transition. The same argument can be applied to the monomeric units in the random copolymer and to the main dielectric relaxation. This is due to the small number of polymer segments that participate in the co-operative rearrangement.

The composition dependence of the position of the main dielectric relaxation in the temperature axis for a given frequency can be determined from the temperature dependence of the frequency of the maxima. This interpolation was made for the frequency of  $10^5$  Hz (a relatively high frequency to eliminate conductivity effects), with the results shown in Figure 2.

The isochronous representation of the dynamic-mechanical results (Figure 7) shows a single loss tangent peak for each copolymer network. The peak shown by PEMA is broader than that of PHEA, and the width of the copolymers seems to increase gradually with their EMA content. The superposition of the dynamic-mechanical isotherms is not perfect in the case of the loss tangent of the PEMA network in the high-frequency region due to the influence of the secondary mechanism in this region. On the other hand, in the case of PHEA, the plot of the  $\log(\tan\delta)$  shows a shoulder on the low-frequency side of the main peak, i.e., corresponding to the high-temperature region in an isochronal peak. This feature is not evident in a linear plot, as can be seen in Figure 7. This may be due to the

presence of cooperative regions in which the mobility of the polymer chains is restricted by the association of the polymer chains through hydrogen bonding. The presence of high- $T_g$  regions in poly(hydroxyethyl methacrylate) networks has already been reported using differential scanning calorimetry [25]. This feature can be also seen in the copolymers, which is more apparent as the HEA content increases.

The parameter  $B$  in the VFTH equation (7) controls the curvature of the Arrhenius diagram and  $D=B/T_0$  is the strength parameter (high values of  $D$  represent "strong" behaviour and low values characterise "fragile" behaviour [30 -32]).

The Vogel temperature  $T_0$ , varies monotonously according to the composition of the copolymer. However, it is interesting to note that the dependence of  $B$  on the composition is by no means monotonous. The value  $B$  is nearly constant for HEA contents up to 50% and then decreases rapidly, meaning that for intermediate compositions the value of  $B$  is higher than that corresponding to a linear dependence on the weight fraction of HEA. These are the copolymers with the highest values of  $D$ , or the smallest fragilities. A correlation between  $B$  and the cooperativity parameter  $n=1-\beta_{KWW}$  (where  $\beta_{KWW}$  is the parameter of the Kohlrausch-Williams-Watts equation or stretched exponential) was proposed within the framework of the coupling model [30,33]. Higher values of  $B$  would correspond to lower values of  $\beta_{KWW}$ , i.e. to broad relaxation processes. The shape of the dynamic-mechanical relaxation process is difficult to analyse quantitatively, but the copolymers with the highest values of  $B$  are those with the broadest dielectric relaxation, characterised by the parameter  $a$  of the Havriliak-Negami equation, as commented above. It seems that the existence of concentration fluctuations produced by the sequence of monomeric units along the copolymer chains also affects fragility.



## 4 Conclusions

The segmental dynamics of P(EMA-co-HEA) random copolymers has been characterised by means of dielectric and dynamic-mechanical relaxation spectroscopy.

A single, narrow main relaxation peak is shown in the copolymers. The characteristic temperature of the  $\epsilon''$  relaxation depends on the copolymer composition according to the Fox equation. A master curve was built for the relative dielectric permittivity curves with accurate superposition. The shape of the  $\epsilon''$  vs frequency plots was analysed with the Havriliak-Negami equation, and it was concluded that the distribution of relaxation times is broader in the copolymers with intermediate composition than in the homopolymers, a feature that can be explained by the inhomogeneity produced on the molecular scale by the sequence distribution of the monomeric units along the chain. This feature may be related to the fact that in the kinetic fragility schema proposed by Angell, the copolymers are stronger than expected in a simple average of the properties of the homopolymers. The strength parameter was determined from the temperature dependence of the dynamic-mechanical relaxation times, which were in turn determined from the shift factors needed to build master curves for the elastic modulus and the loss tangent.

## Acknowledgements

The authors are grateful for the support given by the Spanish Science and Technology Ministry through the MAT2003-05391-C03-01 project and by the Valencian Regional Government (Generalitat Valenciana) through the GRUPOS03/018 project. We would like to thank the R+D+i Linguistic Assistance Office at the Universidad Polit cnica de Valencia for their help in revising this paper.

## References

- [1] M. Gordon, J. S. Taylor, *J. Appl. Chem.* 2 (1952) 493.
- [2] T. G. Fox, *Bull. Am. Phys. Soc.* 1 (1956) 123.
- [3] P. R. Couchman, *Macromolecules* 11 (1978) 1156.
- [4] G. Karanikolopoulos, C. Batis, M. Pitsikalis, N. Hadjichristidis, *J. Polym. Sci. Polym. Chem.* 42 (2004) 3761.
- [5] D. Rana, H. Mounach, J. L. Halary, L. Monnerie, *J. Mat. Sci.* 40 (2005) 943.
- [6] N. W. Johnston, *J. Macromol. Sci. Rev. Macromol. Chem.* 14 (1976) 215.
- [7] J. M. Barton, *J. Polym. Sci. C* 30 (1970) 573.
- [8] M. Salmerón Sánchez, R. Brígido Diego, S. A. M. Iannazzo, J. L. Gómez Ribelles, M. Monleón Pradas, *Polymer* 45 (2004) 2349.
- [9] G. Williams, *Trans. Faraday Soc.* 62 (1966) 2091.
- [10] G. Williams, *Adv. Polymer Sci.* 33 (1979) 60.
- [11] M. Beiner, *Macromol. Rapid. Commun.* 22 (2001) 869.
- [12] D. Gómez, A. Alegría, K. Arbe, J. Colmenero, *Macromolecules* 34 (2001) 503.
- [13] F. Kremer, A Schönhsals eds.; *Broadband Dielectric Spectroscopy*, Springer-Verlag , Berlin, 2003.
- [14] J. M. Meseguer Dueñas, J. Molina Mateo, J.L. Gómez Ribelles, *Polym. Eng. Sci.* 45 (2005) 1336.
- [15] A. Kyritsis, J.L. Gómez Ribelles, J.M. Meseguer Dueñas, N. Soler Campillo, G. Gallego Ferrer, M. Monleón Pradas, *Macromolecules* 37 (2004) 446.
- [16] J. van Turnhout, in: G.M. Sessler (Ed.), *Electrects, Topics in Applied Physics*, vol. 33, Springer, Berlin, 1980, Ch. 3.
- [17] P. Pissis, A. Anagnostopoulou-Konsta, L. Apekis, D. Daoukaki-Diamanti, C. Christodoulides, *J. Non-Cryst. Solids* 131 (1991) 1174.
- [18] P. Pissis, A. Kyritsis, A.A. Konsta, D. Daoukaki, *J. of Molecular Structure* 479 (1999) 163.
- [19] R. Diaz-Calleja, *Macromolecules* 33 (2000) 8924.
- [20] C.J.F. Boettcher, P. Bordewijk, *Theory of Electric Polarization*, 2nd ed., Elsevier, Amsterdam, 1978, Vol. 2.

- [21] S. Havriliak, S. Negami, J. Polym. Sci. C, 14 (1966) 99.
- [22] S. Havriliak, S. Negami, Polymer, 8 (1967) 161.
- [23] J. L. Gómez Ribelles, M. Monleón Pradas, J. M. Meseguer Dueñas, C. Torregrosa Cabanilles, J. Non-Cryst. Solids, 307 (2002) 731.
- [24] J. D. Ferry *Viscoelastic Properties of Polymers*, 3rd ed. New York: John Wiley & Sons, 1980.
- [25] M. Salmerón Sánchez, Y. Touzé, A. Saiter, J.M. Saiter, J.L. Gómez Ribelles, Colloid Polym Sci. 283 (2005) 711.
- [26] G. Williams, D. C. Watts, S. B. Dev, A. M. North, Trans. Faraday Soc. 67 (1971) 1323.
- [27] H. Vogel, Phys. Z. 22 (1921) 645.
- [28] G. A. Fulcher, J. Am. Chem. Soc. 8 (1925) 339.
- [29] G. Tamman, W. Hesse, Z. Anorg. Allg. Chem. 156 (1926) 245.
- [30] R. Böhmer, K. L. Ngai, C. A. Angell, D. J. Plazek, J. Chem. Phys. 99 (1993) 4201.
- [31] C.A. Angell, J Non-Cryst. Solids, 131 (1991) 13.
- [32] C.A. Angell, Annu. Rev. Phys. Chem. 43 (1992) 693.
- [33] D. J. Plazek, K. L. Ngai, Macromolecules 24 (1991) 1222.